The EMBO Journal Vol.18 No.11 pp.2950–2960, 1999

Disease states associated with telomerase deficiency appear earlier in mice with short telomeres

Eloísa Herrera, Enrique Samper, Juan Martín-Caballero, Juana M.Flores[1], Han-Woong Lee[2] and María A.Blasco[3]

Department of Immunology and Oncology, Centro Nacional de Biotecnología-CSIC, Campus Cantoblanco, E-28049 Madrid, [1]Department of Animal Pathology II, Facultad de Veterinaria, Universidad Complutense de Madrid, Madrid, Spain and [2]Samsung Biomedical Research Institute, Songkyunkwan University School of Medicine, Seoul, Korea

[3]Corresponding author
e-mail: mblasco@cnb.uam.es

E.Herrera and E.Samper contributed equally to this work

Mice deficient for the mouse telomerase RNA (mTR$^{-/-}$) and lacking telomerase activity can only be bred for approximately six generations due to decreased male and female fertility and to an increased embryonic lethality associated with a neural tube closure defect. Although late generation mTR$^{-/-}$ mice show defects in the hematopoietic system, they are viable to adulthood, only showing a decrease in viability in old age. To assess the contribution of genetic background to the effect of telomerase deficiency on viability, we generated mTR$^{-/-}$ mutants on a C57BL6 background, which showed shorter telomeres than the original mixed genetic background C57BL6/129Sv. Interestingly, these mice could be bred for only four generations and the survival of late generation mTR$^{-/-}$ mice decreased dramatically with age as compared with their wild-type counterparts. Fifty percent of the generation 4 mice die at only 5 months of age. This decreased viability with age in the late generation mice is coincident with telomere shortening, sterility, splenic atrophy, reduced proliferative capacity of B and T cells, abnormal hematology and atrophy of the small intestine. These results indicate that telomere shortening in mTR$^{-/-}$ mice leads to progressive loss of organismal viability.

Keywords: hematology/infertility/splenic atrophy/telomerase/telomere

Introduction

Telomeres are the ends of eukaryotic chromosomes and, in all vertebrates, consist of tandem repeats of the sequence TTAGGG (for reviews see Blackburn, 1991; Greider, 1996). Telomeres stabilize chromosome ends, preventing end-to-end fusions (Counter *et al*., 1992; Blasco *et al*., 1997; Lee *et al*., 1998; Nakamura *et al*., 1998; Niida *et al*., 1998; Hande *et al*., 1999). Telomerase is a specialized reverse transcriptase that synthesizes telomeric repeats *de novo* (Nugent and Lundblad, 1998). Telomerase is composed of a catalytic protein subunit known as TERT (Harrington *et al*., 1997a; Kilian *et al*., 1997; Lingner *et al*., 1997; Meyerson *et al*., 1997; Nakamura *et al*., 1997; Greenberg *et al*., 1998; Martín-Rivera *et al*., 1998), an RNA molecule or telomerase RNA (TR) that contains the template for the addition of new telomeric repeats (Greider and Blackburn, 1989; Singer and Gottschling, 1994; Blasco *et al*., 1995; Feng *et al*., 1995; McEachern and Blackburn, 1995) and a number of associated proteins (Collins *et al*., 1995; Harrington *et al*., 1997b; Nakayama *et al*., 1997; Gandhi and Collins, 1998).

Telomeric sequences are lost during culture of primary cells and with increasing age in some adult tissues (reviewed in Autexier and Greider, 1996). In particular, telomere lengths in fibroblasts and peripheral blood mononuclear cells (PBMCs) decline proportionally to donor age at a rate of 50–200 bp per year (Harley *et al*., 1990; Vaziri *et al*., 1993). Telomere shortening in adult cells that normally express telomerase, such as those of the hematopietic system, has been proposed to be due to down-regulation of telomerase activity with age (Hiyama *et al*., 1995) and/or to the possibility that the levels of telomerase activity present in those tissues are not sufficient to prevent telomere shortening (Chiu *et al*., 1996). Telomere loss has been proposed to limit the life span of human cells (reviewed in Autexier and Greider, 1996). Recent experiments suggest that telomere length limits the proliferative capacity of cultured cells. In particular, introduction of a constitutively expressed telomerase catalytic subunit into cells with a limited life span is sufficient to stabilize their telomeres and, in some cases, to extend their life span indefinitely without inducing changes associated with transformation (Bodnar *et al*., 1998; Kiyono *et al*., 1998; Wang *et al*., 1998; Jiang *et al*., 1999; Morales *et al*., 1999). These experiments support the notion that telomere length may also play an important role in determining organism life span.

The characterization of mice genetically deficient for the TR component of mouse telomerase, mTR, and therefore lacking telomerase activity, is an important step toward understanding the role of telomerase in telomere maintenance and organism viability (Blasco *et al*., 1997; Lee *et al*., 1998; Herrera *et al*., 1999; Rudolph *et al*., 1999). mTR$^{-/-}$ mice are viable; however, as telomeres shorten and chromosome fusions accumulate with increasing generations, the mTR$^{-/-}$ mice show defects in the reproductive and the hematopoietic system (Blasco *et al*., 1997; Lee *et al*., 1998; Rudolph *et al*., 1999). Here, we show that a variety of disease states associated with mouse aging, such as infertility, splenic atrophy, decreased immune system reactivity, abnormal hematology and small intestine atrophy, appear early in mTR$^{-/-}$ mice on a genetic background with short telomeres.

Results and discussion

Telomere shortening in mTR$^{-/-}$ mice on a C57BL6 background

Mice genetically deficient in the RNA component of telomerase (mTR$^{-/-}$) lack telomerase activity, and mouse embryonic fibroblasts (MEFs) derived from them show telomere loss at a rate of ~3–5 kb per mouse generation up to the sixth generation (G6) (Blasco *et al*., 1997; Hande *et al*., 1999; this study). G6 mTR$^{-/-}$ mice are infertile and show hematopoietic defects, decreased viability and increased tumor incidence in old age (Lee *et al*., 1998; Rudolph *et al*., 1999). To determine whether the time of appearance and the severity of phenotypes in mTR$^{-/-}$ mice correlate with telomere length, we have generated mTR$^{-/-}$ mice on a different genetic background. Previous studies indicated that MEFs from mTR$^{-/-}$ embryos on a C57BL6 background showed significantly shorter telomeres than MEFs derived from mTR$^{-/-}$ embryos on the original mixed C57BL6/129Sv background (Herrera *et al*., 1999). After three backcrosses of the original mTR$^{-/-}$ mice with a pure C57BL6 background, we obtained mTR$^{-/-}$ mice that were ~95% C57BL6 (B6). These mice were interbred to generate increasing generations of mTR$^{-/-}$ mice; interestingly, we were only able to obtain up to four generations (see below).

To determine telomere length in the B6 mTR$^{-/-}$ mice, we performed quantitative fluorescent *in situ* hybridization (Q-FISH) in both MEFs and bone marrow cells isolated from mice of different generations. Bone marrow cells were included in the analysis because some of the phenotypes that emerge in mTR$^{-/-}$ mice affect the hematopoietic system (Lee *et al*., 1998; this study). Telomere length was estimated by the fluorescence intensity of the telomeres (see Materials and methods for details). Q-FISH analysis showed that the average telomere fluorescence of p- and q-telomeres decreases with increasing generations of mTR$^{-/-}$ mice on the B6 background, indicating an average rate of telomere shortening of 4.92 and 3.80 kb per generation for MEFs and bone marrow cells, respectively (calculated as described in Figure 1A; see Table I for Q-FISH data and Figure 1B for histograms showing the increased frequencies of short telomeres in late generation B6 mTR$^{-/-}$ bone marrow cells). In parallel, we carried out Q-FISH analysis of MEFs and bone marrow cells derived from wild-type, G3 and G6 mTR$^{-/-}$ mice in the mixed background (Table I). Mixed background mTR$^{-/-}$ MEFs showed a rate of telomere shortening of ~3.3 kb per generation (Table I) similar to that previously described (Blasco *et al*., 1997; Hande *et al*, 1999). Interestingly, the average telomere length of mixed background bone marrow cells did not decrease as predicted (Table I), despite the fact that these cells showed an increase in the frequency of short telomeres with increasing generations (Figure 1C), as previously described for B6 bone marrow cells (Figure 1B). The apparent lack of shortening in the mixed background bone marrow cells could be due to a higher frequency of very long telomeres (>120 kb) in G3 and G6 mixed background cells (Figure 1C) than in the G4 B6 cells. Telomere shortening in B6 mTR$^{-/-}$ mice resulted in G3 MEFs and G4 bone marrow cells with average telomere lengths of 21.88 ± 14.64 and 20.88 ± 14.52 kb, respectively, shorter than the average telomere lengths of G6 mixed background cells (Table I). Coincident with telomere shortening, B6 mTR$^{-/-}$ cells showed an increase in the number of telomeres without detectable TTAGGG repeats from 0% in the wild-types to 8.67 and 7.00% in the G3 MEFs and G4 bone marrow cells, respectively; again, higher frequencies than in the G6 mixed background cells (Table I). An increase in the number of end-to-end fusions per metaphase was also detected in the G3 B6 mTR$^{-/-}$ MEFs and G4 bone marrow cells as compared with G6 mixed background mTR$^{-/-}$ cells (Table I). In summary, this study shows that at different mTR$^{-/-}$ generations, the average length of telomeres was significantly shorter in the B6 than in the mixed background cells (Table I); this resulted in G3 and G4 B6 mTR$^{-/-}$ cells with shorter telomeres and higher chromosomal instability than G6 mixed background mTR$^{-/-}$ cells. These observations are in agreement with the fact that G3 and G4 B6 mTR$^{-/-}$ mice show stronger phenotypes associated with telomerase deficiency than the G6 mixed background mTR$^{-/-}$ mice (this study).

mTR$^{-/-}$ mice on a C57BL6 background can be bred for only four generations

We previously described that the matings of mTR$^{-/-}$ mice on a mixed C57BL6/129Sv background were productive to the fifth (Lee *et al*., 1998) or, in some cases, to the sixth generation (unpublished results), and that we obtained only six or seven generations, respectively, of mTR$^{-/-}$ mice (Lee *et al*., 1998). In addition, there was a progressive

Fig. 1. Telomere shortening in mTR$^{-/-}$ mice on two different genetic backgrounds. (**A**) Separate telomere fluorescence of the p-arm and q-arm, and that of the average of both, from primary MEFs and bone marrow cells derived from wild-type and mTR$^{-/-}$ B6 mice of the indicated generations. Fluorescence is expressed in telomere fluorescence units (TFU), where 1 TFU corresponds to 1 kb of TTAGGG repeats in plasmid DNA (Martens *et al*., 1998). Each value represents the mean of 10–15 metaphases. Primary MEFs and B6 bone marrow cells from wild-type (wt) and several mTR$^{-/-}$ B6 embryos from the first (G1), second (G2) and third generation (G3) were used (see Table I for Q-FISH data). The standard deviation is indicated by bars. Notice that we chose to represent standard deviation rather than standard error. Typically, standard deviation for mouse telomere length is ~15 kb and this value is independent of the number of metaphases analyzed (Blasco *et al*., 1997). In contrast, and because of the large number of data points in Q-FISH analysis, the standard error of mean telomere fluorescence estimates is very small (<0.5 kb for 10–15 metaphases) despite considerable variation in individual telomere fluorescence values (standard deviation). The average combined telomere length of q- and p-telomeres in the different samples studied from each generation was plotted and the data analyzed by the least squares methods to calculate the average telomere shortening per generation; the r^2 values close to 1 indicate that adjusting the data to a linear equation is correct. We determined a telomere shortening of 4.92 and 3.80 kb per generation for MEFs and bone marrow cells, respectively. (**B**) Frequency of telomere fluorescence intensity values of the average of p- and q-telomeres (black bars) in bone marrow cells derived from wild-type and several B6 mTER$^{-/-}$ mice from the second (KO-G2a and KO-G2b), third (KO-G3a and KO-G3b) and fourth generation (KO-G4). The frequency of chromosomes with short telomeres increases with the increasing generations. (**C**) Frequency of telomere fluorescence intensity values of the average of p- and q-telomeres (black bars) in bone marrow cells derived from wild-type and mixed background mTR$^{-/-}$ mice from the third (KO-G3) and sixth generation (KO-G6). The frequency of chromosomes with short telomeres increases with the increasing generations; however, a larger heterogeneity is observed in the mixed than in the B6 background. The distribution of telomere fluorescence in G4 B6 mTR$^{-/-}$ bone marrow cells is shown again to facilitate comparison.

decrease in litter size in the mTR$^{-/-}$ mixed background mice with each additional generation of mTR$^{-/-}$ mice. This decline in litter size has been attributed both to male and female infertility and to increasing embryonic death due to a neural tube closure defect (Lee *et al*., 1998; Herrera *et al*., 1999). Interestingly, mTR$^{-/-}$ mice on a 95% C57BL6 genetic background are fertile only to the third generation, and no progeny were produced when matings of G4 mTR$^{-/-}$ B6 animals were carried out; in fact, there was a 60% decline in the litter size in B6 G3 intercrosses (Figure 2A). This decline is due to embryonic death as a consequence of a neural tube closure defect in the mTR$^{-/-}$ B6 mice (Herrera *et al*., 1999), as well as to infertility (this study). The G3 mTR$^{-/-}$ B6 mice show testicular

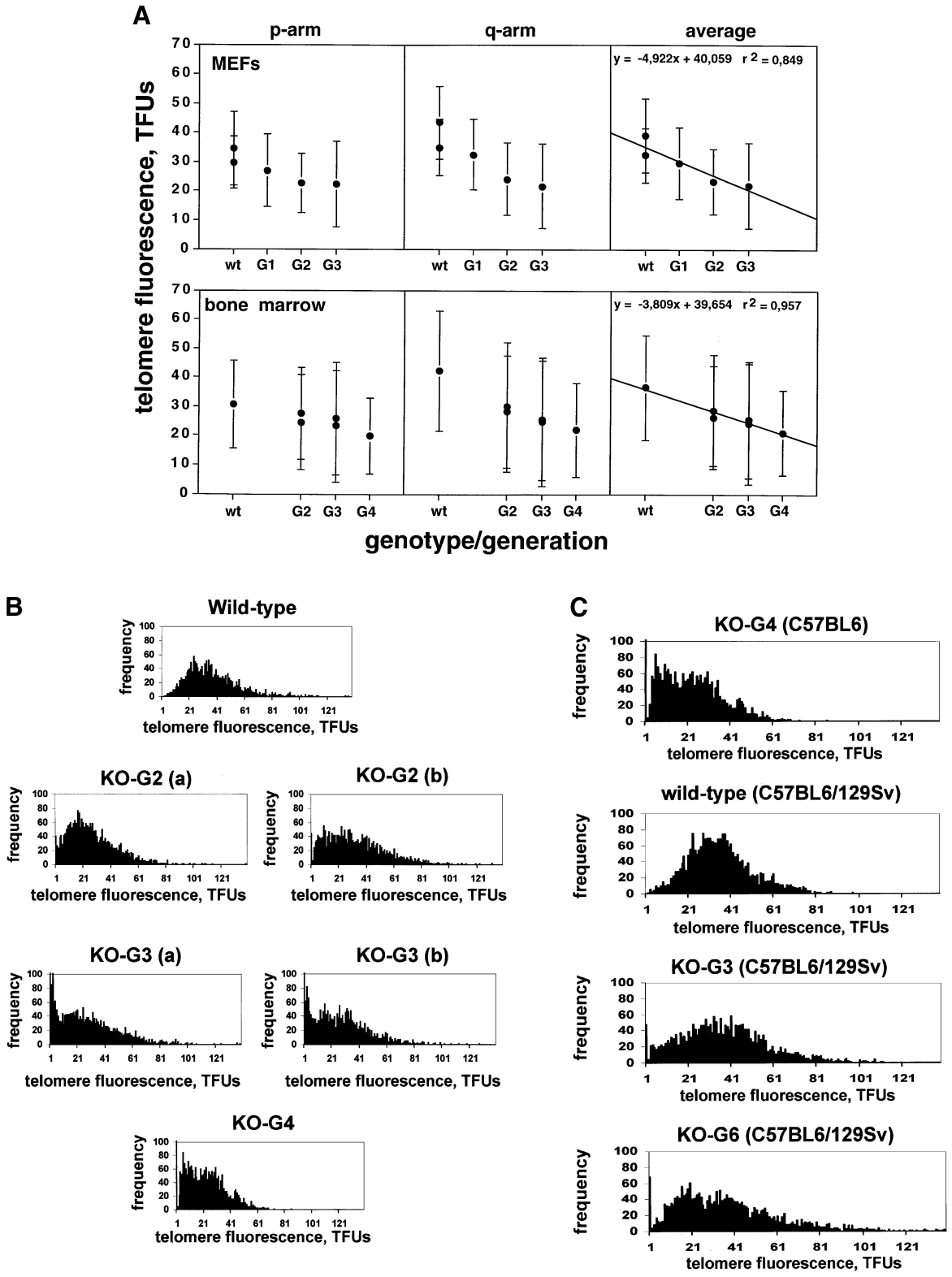

Table I. Telomere length analysis of wild-type and mTR$^{-/-}$ mice in two different genetic backgrounds

Genotype	Telomere fluorescence (TFU)			No. of metaphases	Fusions per metaphase	Telomeres lacking TTAGGG (%)
	p-arm	q-arm	p + q			
MEFs						
Wild-type[a] C57BL6	29.71 ± 8.84	34.94 ± 9.68	32.32 ± 9.27	15	0.0	0.4
Wild-type[b] C57BL6	34.48 ± 12.52	43.51 ± 12.44	38.99 ± 12.48	10	0.0	0.11
KO-G1 C57BL6	26.91 ± 12.37	32.40 ± 12.06	29.65 ± 12.21	10	0.0	1.44
KO-G2 C57BL6	22.51 ± 10.15	24.11 ± 12.34	23.31 ± 11.23	10	0.0	2.50
KO-G3[a] C57BL6	22.14 ± 14.68	21.63 ± 14.59	21.88 ± 14.64	10	0.6	8.67
Wild-type[a] C57BL6/129Sv	41.76 ± 13.43	55.56 ± 18.47	48.66 ± 15.95	11	0.1	0
Wild-type[b] C57BL6/129Sv	36.84 ± 10.76	45.80 ± 14.24	41.32 ± 12.50	10	0.0	0.25
KO-G3[a] C57BL6/129Sv	24.16 ± 12.89	28.55 ± 16.36	26.36 ± 14.63	11	0.0	1.53
KO-G3[b] C57BL6/129Sv	26.93 ± 12.65	41.22 ± 14.01	34.08 ± 13.31	11	0.0	1.18
KO-G6[a] C57BL6/129Sv	21.50 ± 16.13	30.24 ± 17.45	25.87 ± 16.79	10	0.4	6.49
KO-G6[b]	19.39 ± 13.09	30.98 ± 13.93	25.18 ± 13.51	10	0.3	6.77
Bone marrow cells						
Wild-type C57BL6	30.68 ± 15.15	42.22 ± 20.70	36.45 ± 17.92	11	0.06	0
KO-G2[a] C57BL6	24.37 ± 16.25	28.08 ± 19.21	26.23 ± 17.73	15	0	1.58
KO-G2[b] C57BL6	27.52 ± 15.86	29.84 ± 22.15	28.68 ± 19.00	14	0.066	1.92
KO-G3[a] C57BL6	23.11 ± 19.04	24.80 ± 22.02	23.96 ± 20.53	15	0.066	6.51
KO-G3[b] C57BL6	25.84 ± 19.28	25.24 ± 20.45	25.54 ± 19.96	14	0.21	5.63
KO-G4 C57BL6	19.92 ± 12.92	21.85 ± 16.12	20.88 ± 14.52	15	0.27	7.00
Wild-type C57BL6/129Sv	27.35 ± 11.50	42.20 ± 14.95	34.77 ± 13.23	15	0	0
KO-G3 C57BL6/129Sv	25.91 ± 14.05	45.54 ± 21.98	35.73 ± 18.02	14	0.07	2.16
KO-G6 C57BL6/129Sv	24.97 ± 16.55	46.68 ± 25.19	35.83 ± 20.92	15	0.86	2.76

[a,b]Two different mice from the same generation.

atrophy as well as a depletion of male germ line cells (Figure 2B–E), similar to the previously described defect in G6 mTR$^{-/-}$ mice in the mixed C57BL6/129Sv background. Testes from G3 mTR$^{-/-}$ B6 mice are 60% lighter relative to their body weight than the wild-type testes (Figure 2B, see also Figure 2C for an example). Wild-type testes show normal testicular structure and spermatogenesis (Figure 2D); in contrast, histology of age-matched G3 mTR$^{-/-}$ B6 testes revealed various abnormalities: (i) the epithelium is markedly depleted of germ cells and lined only by vacuolated Sertoli cells; (ii) the lumen of atrophied tubules is filled with a concentric nest of cells composed of amorphous cellular detritus and released degenerated cells; and (iii) the basement membrane around the atrophic tubules is thicker than in the wild-type testes (all the lesions are represented in Figure 2E). Interestingly, a marked hyperplasia of the Leydig cells was also observed, in agreement with the higher incidence of testicular tumors in the mixed background mTR$^{-/-}$ from late generations (Rudolph *et al*., 1999). These lesions are similar to those that occur in individuals affected with the 'Sertoli cell-only syndrome' (Nistal *et al*., 1982). In normal mice, identical lessions have been described as a regressive change observed in 40% of mice of 15–17 months of age (Takano and Abe, 1987).

Reduced size of mTR$^{-/-}$ mice on the C57BL6 background

We observed that adult G3 mTR$^{-/-}$ B6 mice were significantly smaller than age-matched wild-type B6 mice (see Figure 3A, and 3B for an example). Although some newborn G3 mTR$^{-/-}$ B6 mice were smaller than age-matched wild-type B6 mice, there was on average no significant size difference between G3 mTR$^{-/-}$ and wild-type mice (see Figure 3A) before 4 months of age. However, as both G3 mTR$^{-/-}$ B6 males and females aged, a weight difference of 20% became apparent in animals older than 4 months (Figure 3A and B). A similar reduction in weight was observed for the few G4 mTR$^{-/-}$ B6 mice obtained (not shown). This reduction in weight and size

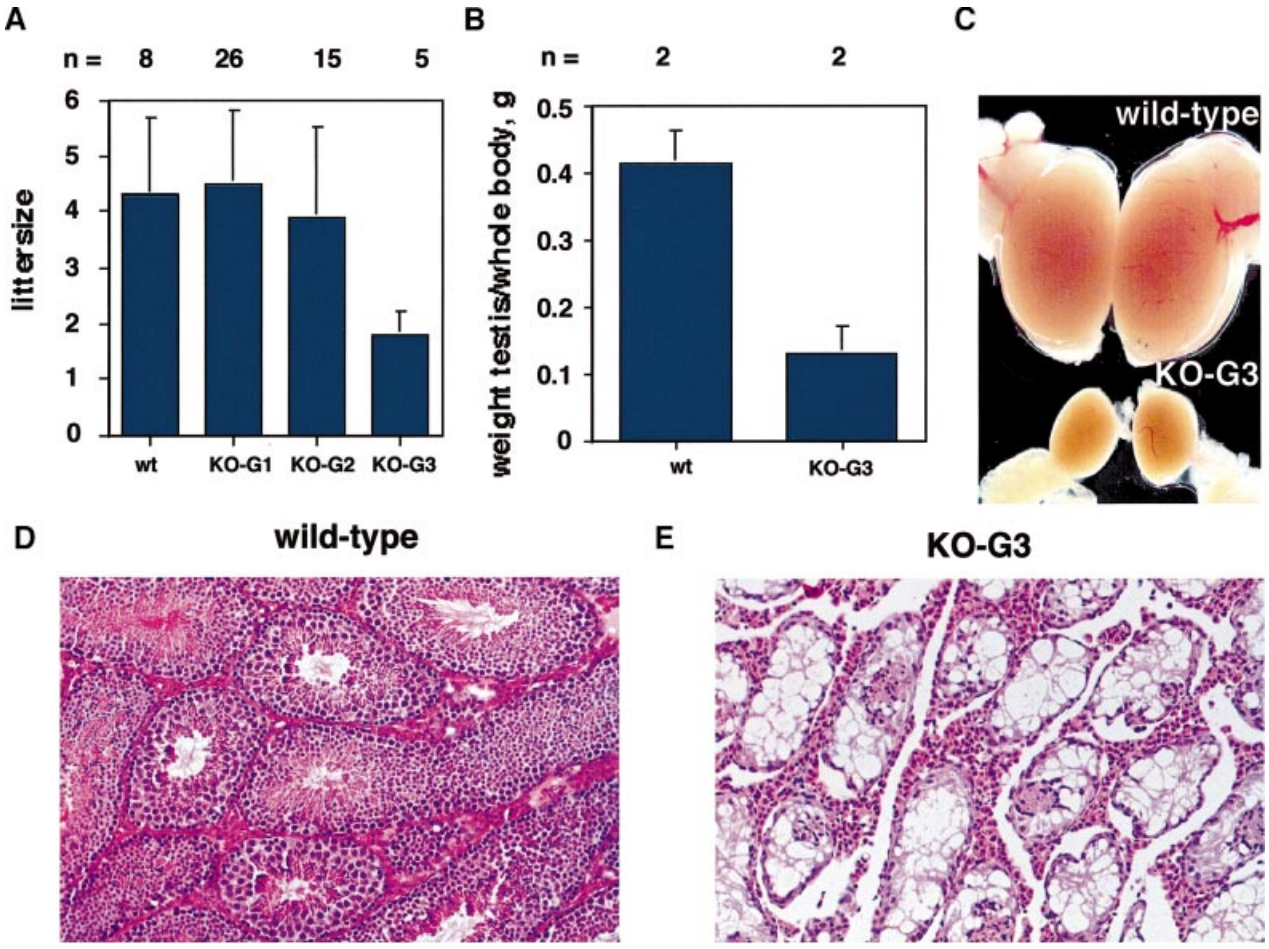

Fig. 2. mTR$^{-/-}$ mice in a C57BL6 background are viable for only four generations. (**A**) The average progeny per litter of different generations of wild-type or mTR$^{-/-}$ crosses is shown with bars. The total number of crosses of each genotype used for the analysis is indicated at the top of the graph. Wt, wild-type; G1 to G3 indicate the generations of the mTR$^{-/-}$ mice used in the crosses. Standard deviation bars are shown. (**B**) The average weight of testes relative to body weight is plotted for wild-type (wt) and G3 mTR$^{-/-}$ (B6) testes (KO-G3). The total numbers of mice used in the study are indicated above the graph. Standard deviation bars are shown. (**C**) Representative images of testes from an age-matched wild-type and a G3 mTR$^{-/-}$ B6 mouse (7 months old). (D and E) Histology of a wild-type (**D**) and a G3 mTR$^{-/-}$ B6 (**E**) testis. The figure shows the abnormal histology of the G3 testis compared with that of the wild-type. No precursor cells or spermatids were detected in the G3 B6 testis.

coincides with an increase in the percentage of deaths in the colony (see below), as well as with a general impoverishment of the health of the mice (see below). The cause of the reduced body weight remains unknown; however, it is tempting to speculate that it could be a consequence of the atrophy of the small intestine in these animals (see below).

Decreased viability with age of mTR$^{-/-}$ mice on the C57BL6 background coincides with the appearance of hematopoietic system defects and small intestine atrophy

Whereas G6 mTR$^{-/-}$ mice on the mixed C57BL6/129Sv background showed decreased viability only at advanced ages [>18 months in the colony studied by Rudolph *et al*. (1999) and 7 months in our mixed background colony (Figure 3C)], there was a dramatic loss of viability with increasing age in the G3 and G4 mTR$^{-/-}$ B6 mice. In particular, 50% of the G4 mice had died by 5 months after birth, and only 30% survived longer than 8 months (Figure 3D). In G3 mTR$^{-/-}$ B6 mice, mortality was 15% in animals at 1 year of age, whereas no death was observed in age-matched wild-type mice (Figure 3D).

Due to the difficulty in obtaining G4 mTR$^{-/-}$ B6 mice, we investigated the possible causes of reduced viability using G3 mTR$^{-/-}$ B6 mice under 1 year of age at the time of death. In ~40% of the cases, the cause of death could not be determined precisely. Gross studies showed no patent abnormalities and the mice showed no signs of disease prior to death. In particular, histological analysis of the heart and the brain revealed no abnormality, although we cannot rule out stroke or any other cardiovascular problems as the cause of these asymptomatic deaths. In 60% of the cases, death occurred within 48 h of detecting signs of poor health, including reduced activity, lowered responsiveness to stimuli, bristly hair, dehydrated skin, a hunched position and small size. To address the possible cause of death in the B6 colony, we sacrificed G3 mTR$^{-/-}$ B6 mice showing these signs before death occurred. Once again, histological analysis of heart and brain revealed no abnormalities (not shown); however, we detected a variety of defects in the small intestine, as well as spleen atrophy, a decreased mitogenic response by B and T cells and abnormal blood cell counts.

The small intestine. In all the G3 mTR$^{-/-}$ B6 mice showing

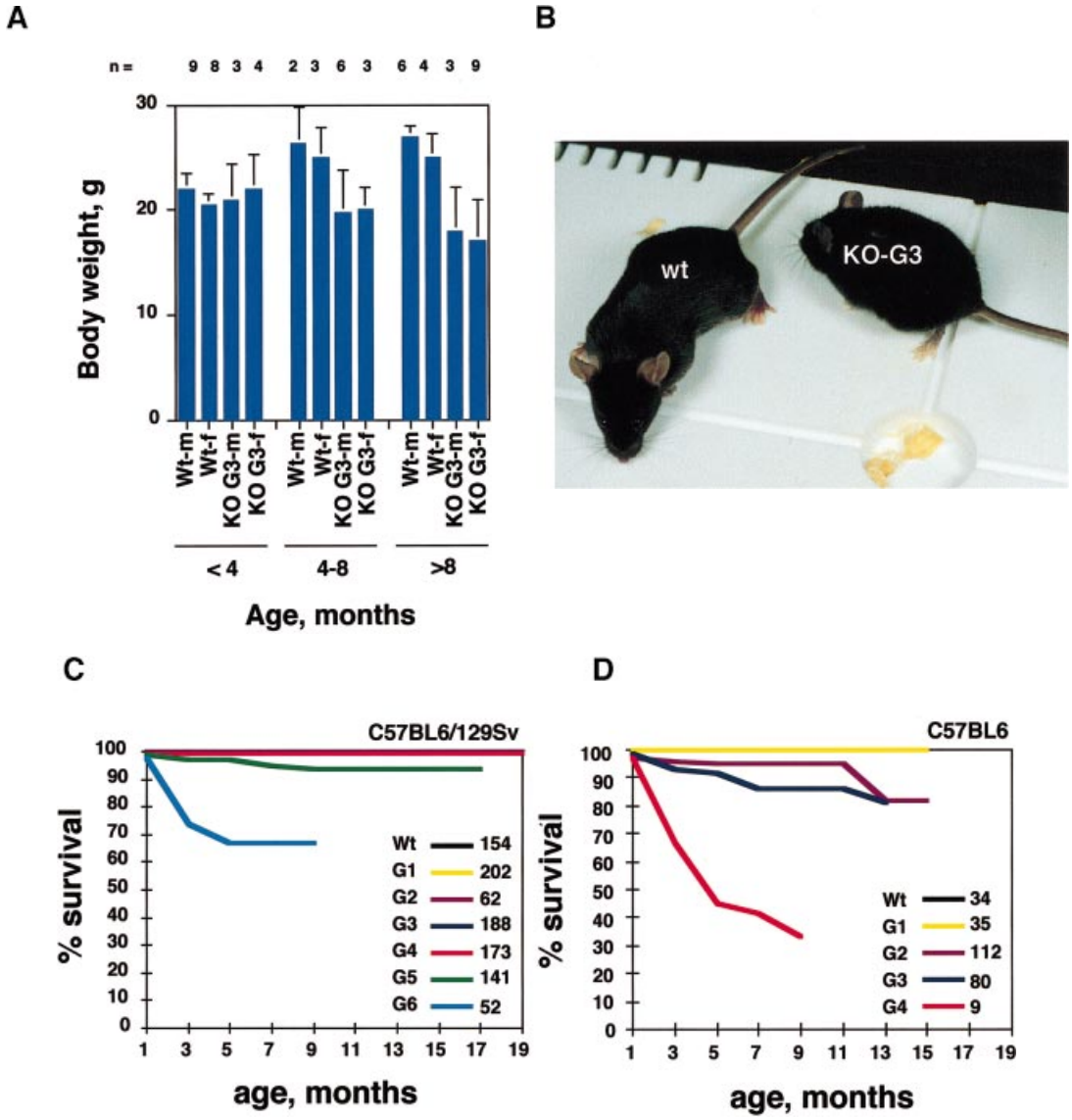

Fig. 3. Reduced body size of G3 mTR$^{-/-}$ B6 mice. (**A**) The average body weights are shown of wild-type and G3 mTR$^{-/-}$ B6 males and females at different ages. The total numbers of mice used are indicated above the graph. Wt-m, wild-type male; Wt-f, wild-type female; KO G3-m, mTR$^{-/-}$ male from the third generation; KO G3-f, mTR$^{-/-}$ female from the third generation. Standard deviation bars are shown. (**B**) Representative images of an age-matched (7 months) wild-type and a G3 mTR$^{-/-}$ mouse on the B6 background. (**C**) Survival of wild-type and mTR$^{-/-}$ mice from different generations. The numbers of mice from each generation are indicated. Black lane, wild-type (wt); yellow lane, first generation (G1); brown lane, second generation (G2); dark blue, third generation (G3); red, fourth generation (G4); green, fifth generation (G5); light blue, sixth generation (G6). (**D**) Survival of wild-type and mTR$^{-/-}$ mice from different generations. The number of mice from each generation are indicated. Black lane, wild-type (wt); yellow lane, first generation (G1); brown lane, second generation (G2); dark blue, third generation (G3); red, fourth generation (G4).

poor health, but not in age-matched wild-type mice, histological analysis of the small intestine revealed various abnormalities. Figure 4A shows a section of a healthy small intestine with normal number and distribution of villi and glands. Figure 4B shows a representative image of the small intestine of a 12-month-old G3 mTR$^{-/-}$ mouse showing signs of poor health. The section shows villous atrophy with shortening of the villi and mucosa flattening in some areas, as well as epithelial and glandular hyperplasia with cystic dilations in other areas (yellow arrows, Figure 4B). Some glandular lumen shows hyaline transformation with crystalline structures (white arrow, Figure 4B). Scattered trinucleated epithelial active cells were also observed frequently at higher magnifications (not shown). These histological alterations have been described as typical age-related lesions in old C57Bl6/C3H hybrids (>2 years old) (Mohr *et al.*, 1996). The abnormal mucosa of the G3 mTR$^{-/-}$ B6 mice might result in a reduced absorption of nutrients and could account for the decreased body weight, dehydrated skin, bristly hair and hunched position that occur in the affected G3 mTR$^{-/-}$ B6 mice. In agreement with this, lymphangiectasia (a lymphatic vessel is indicated by a red arrow in Figure 4B) and increased numbers of lymphocytes and plasma cells are observed in the affected intestines, typical signs of malabsorption syndrome. Hyperplasia of the mucosa could also be a compensatory mechanism to increase the absorption of the affected areas. In some of the histological sections, we detected ulcerations as well as initial stages of peritonitis which might result in the rapid death of the

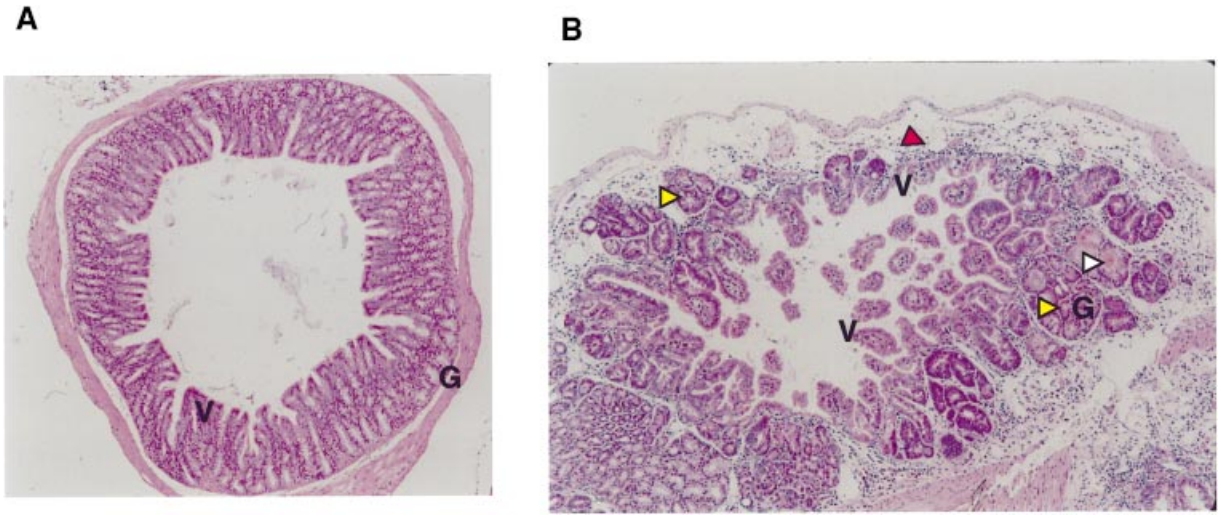

Fig. 4. Small intestine atrophy in G3 mTR$^{-/-}$ B6 mice. (**A**) Transversal section of a normal small intestine from a 12-month-old mouse. Notice the normal number and distribution of the villi (V) and the glands (G). (**B**) Representative image of a transversal section of a small intestine from a 12-month-old G3 mTR$^{-/-}$ B6 mouse showing signs of poor health. Notice areas of atrophy as well as areas of hyperplasia. Hyaline structures and glandular nests are indicated with white or yellow arrows, respectively. A lymphatic vessel is indicated with a red arrow.

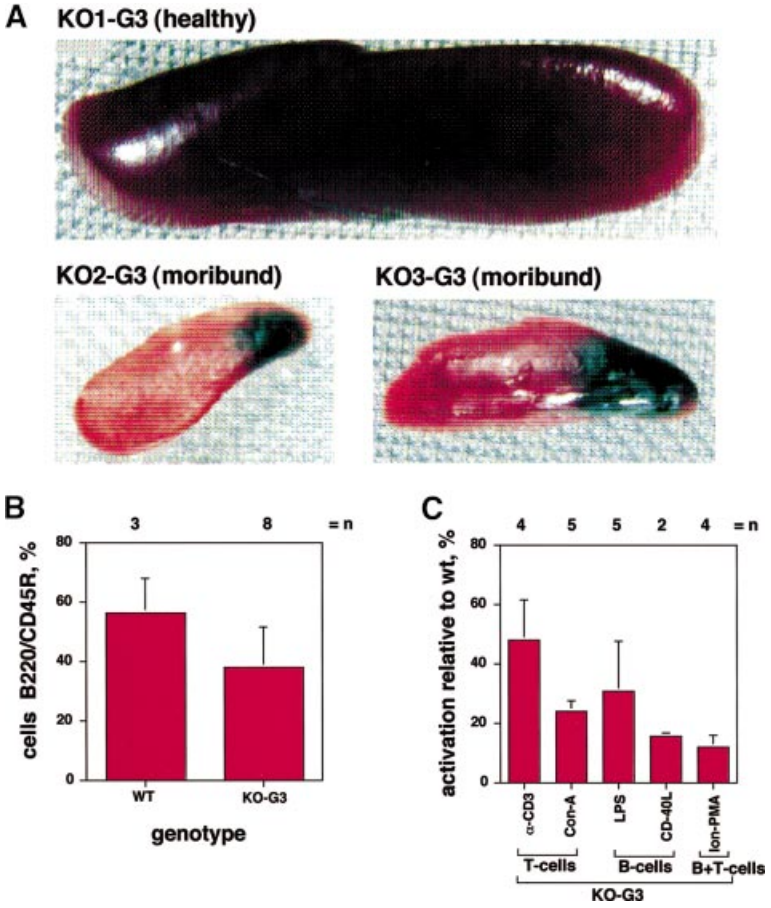

Fig. 5. Spleen dysfunction in G3 mTR$^{-/-}$ B6 mice. (**A**) Images of spleens from two moribund G3 mTR$^{-/-}$ mice (KO2-G3 and KO3-G3) and one healthy G3 mTR$^{-/-}$ mouse (KO1-G3). (**B**) Percentage of total spleen cells positive for the B220/CD45R surface marker. Wt, wild-type splenocytes; KO-G3, splenocytes derived from G3 mTR$^{-/-}$ B6 mice. The total number of mice used for each study is indicated above the graph (n). Standard deviation bars are shown. (**C**) Relative activation with respect to the wild-type following mitogen stimulation of splenocytes from G3 mTR$^{-/-}$ mice. α-CD3 and Con-A, T cell-specific mitogens; LPS and CD-40L, B cell-specific mitogens; Ion-PMA, B + T cell mitogens. The total number of mice used for each experiment is indicated above the graph. Standard deviation bars are shown.

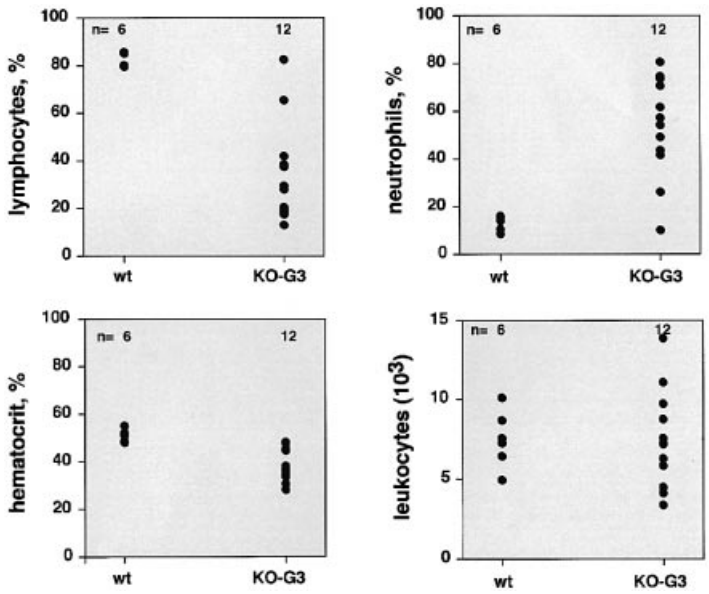

Fig. 6. Hematology of wild-type and G3 mTR$^{-/-}$ mice in a C57BL6 background. Graphs showing total counts of lymphocytes, neutrophils, leukocytes and hematocrit in blood samples from six wild-type and 12 G3 mTR$^{-/-}$ B6 mice. Wild-type mice ranged from 3 to 12 months of age, G3 mTR$^{-/-}$ B6 mice ranged from 9 to 12 months. The total numbers of mice used are indicated on the upper part of the graphs. Wt, wild-type; KO-G3, G3 mTR$^{-/-}$ B6 mice.

affected mice. The small intestine epithelium is completely regenerated every 4–5 days (Stevens and Lowe, 1997); hence, telomere shortening associated with cell division might result in a growth impairment of the epithelial cells, triggering the alterations described above.

The spleen. No histological abnormalities were reported in spleens from mixed background G6 mTR$^{-/-}$ mice (Lee *et al*., 1998). Analysis of spleens from 12-month-old G3 mTR$^{-/-}$ B6 mice revealed diminished organ size in animals showing poor health as compared with healthy mice. Figure 5A shows the spleens of two moribund G3 mTR$^{-/-}$ B6 mice and that of one healthy counterpart. Fluorescence-activated cell sorting (FACS) analysis of splenocytes derived from the affected spleens showed lower numbers of cells positive for the B cell marker B220/CD45R than in the wild-type spleens (Figure 5B), indicating a decrease in the total B cell number in affected spleens. No significant differences in T cell numbers were observed between G3 mTR$^{-/-}$ and wild-type spleens (not shown). Moreover, these splenocytes were impaired in their proliferative response to B- [lipopolysaccharide (LPS) and CD4OL], T- (α-CD3 and concanavalin A) and B + T cell- [ionomycin and phorbol 12-myristate-13-acetate (PMA)] specific mitogens (Figure 5C), indicating a lower proliferative capacity of both T and B cells, as previously described for G6 mTR$^{-/-}$ mice on the mixed background (Lee *et al*., 1998). These results point to an immunological defect as one of the possible causes of poor health and death in G3 mTR$^{-/-}$ B6 mice. Immunosenescence is regarded as one of the landmarks of human aging (Wick and Grubeck-Loebenstein, 1997). It is widely reported that immune system function declines with increasing age; in particular, as humans age, there is a decrease in T cell numbers as well as impaired responsiveness to mitogens (Wick and Grubeck-Loebenstein, 1997).

Hematology. No abnormalities in blood cell counts were reported previously for the G6 mTR$^{-/-}$ mice on the mixed genetic background (Lee *et al*., 1998). Extensive hematological analysis of the G3 mTR$^{-/-}$ B6 colony showed large differences in total lymphocyte and neutrophil numbers (Figure 6; Table II) in G3 mTR$^{-/-}$ mice as compared with wild-type controls. In particular, with the exception of only two animals, all G3 mTR$^{-/-}$ mice showed reduced numbers of lymphocytes compared with age-matched wild-type controls (Figure 6; Table II), concurring with the previously described reduction in spleen B lymphocytes. In the mice with a reduction in lymphocytes, there was also a dramatic increase in neutrophil numbers (Figure 6; Table II) which was not found in the two mice with a normal lymphocyte count (Table II). The increase in neutrophils may be a compensatory mechanism triggered by the low number of lymphocytes. Neutrophils may be compensating for a poor immune response by G3 mTR$^{-/-}$ B6 mouse lymphocytes. We ruled out that the increase in neutrophil numbers could be a consequence of a bacterial infection since the colony is free from viral and bacterial pathogens. Similar increased neutrophil numbers have been described in 27-month-old animals (Smith, 1994). No large differences were detected in total leukocyte numbers or in hematocrit between G3 mTR$^{-/-}$ and the wild-type animals, although the G3 mTR$^{-/-}$ mice generally had a lower hematocrit than the wild-type mice (Table II).

The animals used for hematological analyses were observed for a period of up to 2 months after the blood extraction; Table II indicates the animals that died or showed symptoms of poor health in that time period. It did not escape our attention that the animals showing aberrant blood cell counts were those that showed symptoms of poor health or that died, suggesting a hematological defect as a possible factor contributing to some deaths.

Table II. Hematology of wild-type and G3 mTR$^{-/-}$ B6 mice

Genotype	Age (months)	Hematocrit (%)	Neutrophils (%)	Leukocytes (10^3)	Lymphocytes (%)	Two months after analysis
Wild-type	3	51.8	8.4	8.7	85.3	alive
Wild-type	3	48.0	13.6	4.9	79.4	alive
Wild-type	9	50.8	14.0	10.1	79.8	alive
Wild-type	9	54.6	15.5	7.6	80.0	alive
Wild-type	9	51.3	15.9	6.4	79.8	alive
Wild-type	12	48.4	10.5	7.2	85.0	alive
KO-G3	9	47.1	43.2	8.7	37.1	alive
KO-G3	10	47.8	61.2	7.2	20.5	dead in cage
KO-G3	10	34.1	54.0	11.0	29.2	alive
KO-G3	10	36.0	70.4	4.1	18.3	moribund (sacrificed)
KO-G3	10	33.4	41.1	13.8	41.8	dead in cage
KO-G3	12	37.6	80.4	4.4	12.8	moribund (sacrificed)
KO-G3	12	47.7	48.6	7.6	38.1	moribund (sacrificed)
KO-G3	12	36.2	74.4	3.6	17.5	moribund (sacrificed)
KO-G3	12	44.3	25.7	5.8	65.1	alive
KO-G3	12	44.7	57.0	9.7	27.7	dead in cage
KO-G3	12	27.7	10.0	7.2	82.1	alive
KO-G3	13	30.4	73.3	6.2	19.1	alive

Concluding remarks

The analysis of mTR$^{-/-}$ B6 mice points to a possible role for telomere length in a variety of disease states that are associated with organismal aging in the mouse. The fact that similar phenotypes (i.e. infertility and immune system defects) emerged in mTR$^{-/-}$ mice on two different genetic backgrounds suggests that these phenotypes are strain independent and may be representative of the consequences of telomere shortening in man and other mammals. Most importantly, we describe a number of novel disease states associated with telomere shortening, such as splenic atrophy, abnormal blood cell counts and small intestine atrophy, that might account for the decreased viability of the mTR$^{-/-}$ mice in the B6 background. Finally, the results presented here show that the phenotypes associated with telomerase deficiency appear earlier in genetic backgrounds that have shorter telomeres. This further supports the idea that these phenotypes appear as a consequence of telomere loss and, most importantly, suggests that in mammals with much shorter telomeres, such as man, telomere shortening with age (Harley *et al*., 1990; Vaziri *et al*., 1993) may contribute to the loss of organismal viability that occurs with aging.

Materials and methods

MEF and bone marrow cultures

Primary embryonic fibroblasts from 13.5-day-old wild-type or mTR$^{-/-}$ embryos from several generations were harvested following a 4–5 h treatment with colcemid (0.1 μg/ml), then harvested by centrifugation (120 *g*, 8 min).

Bone marrow cells were obtained by flushing the femora with sterile phosphate-buffered saline (PBS) using a 25 gauge needle. The cell culture was established in MyeloCult 5300 medium (Stem Cell Technologies) containing 12.5% horse serum and 12.5% fetal bovine serum (FBS), supplemented with 20% WEHI cell-conditioned medium containing interleukin (IL)-3, recombinant human IL-6 (200 ng/ml), stem cell factor (50 ng/ml) and erythropoietin (3 μg/ml). The cytokines were a generous gift from Drs Antonio Bernard and Miguel Aracil (CNB, Madrid, Spain). Four days after extraction, bone marrow cells were treated with colcemid (0.1 μg/ml) for 2 h, then harvested by centrifugation (120 *g*, 8 min)

Q-FISH

After hypotonic swelling in 0.03 M sodium citrate for 25 min at 37°C, bone marrow cells and MEFs were fixed in methanol:acetic acid (3:1). After 2–3 fixative changes, the cell suspension was dropped onto clean, wet microscope slides and dried overnight. FISH was performed essentially as described (Zijlmans *et al*., 1997) with minor modifications. Briefly, slides were washed with PBS and fixed for 2 min in 4% formaldehyde. Slides were washed three more times with PBS and treated with pepsin (1 mg/ml, pH 2.0) at 37°C for 10 min. Formaldehyde fixation and washing steps were repeated, slides were incubated in 0.4 M HCl for 10 min, rinsed in PBS, dehydrated in an ethanol series (70, 90 and 100%) and air dried.

The Cy-3-labeled $(C_3TA_2)_3$ PNA probe (Perseptive Biosystems, Bedford, MA) was dissolved in a hybridization buffer containing 70% formamide/10 mM Tris pH 7.0 and 0.25% (w/v) blocking reagent (0.5 μg/ml) (Dupont, Boston, MA). The hybridization mixture was placed onto the slides and a coverslip (22×60 mm) was applied, followed by DNA denaturation (3 min, 80°C). After hybridization (2 h, room temperature), slides were washed twice with 70% formamide/10 mM Tris pH 7.2 for 15 min, followed by a 5 min washing in 0.05 M Tris/0.15 M NaCl pH 7.5/0.05% Tween-20. Slides were dehydrated in an ethanol series and air dried. Finally, slides were counterstained with 4′,6-diamidino-2-phenylindole (DAPI; 0.2 μg/ml) in Vectashield (Vector Laboratories, Burlingame, CA).

Quantitative image analysis

Digital images were recorded with a COHU High Performance CCD camera model 49-12-5000 on a Leica Leitz DMRB fluorescence microscope (Leica, UK) equipped with a red fluorescence filter (Leica I3-513808) and a DAPI fluorescence filter (Leica A-513808) both located on a manual wheel. Images were acquired with the Q-FISH software package (Leica Imaging Systems, UK), using a 100×/NA 1.0 objective lens (Leica) and a 100 W mercury/xenon lamp (Leica). A dedicated computer program was used for image analysis as described previously (Zijlmans *et al*., 1997). The integrated fluorescence intensity for each telomere was calculated after correction for image acquisition exposure time. A minimum of 10 metaphases per group was analyzed. Each metaphase of 40 chromosomes (in the mouse) yields 160 telomere spots, and a typical analysis of 10–15 metaphases produces several thousand telomere fluorescence values. Because of the large number of data points in Q-FISH analysis, the standard error of mean telomere fluorescence estimates is typically small (for example, less than a few percent of the average) despite considerable variation in individual telomere fluorescence values. For this reason, we chose to represent in the graphs the standard deviation rather than standard error.

Calibration. The details of calibration for telomere fluorescence are explained elsewhere (Martens *et al*., 1998). Briefly, we used two calibration levels to ensure reliable quantitative estimation of telomere length in various samples. First, to correct for daily variations in lamp intensity and alignment, images of fluorescent beads were acquired and analyzed with the Image Analysis computer program. Secondly, relative TFUs were extrapolated from the plasmid calibration. For this, we hybridized and analyzed plasmids with a defined $(TTAGGG)_n$ length of

0.15, 0.40, 0.80 and 1.60 kb (Hanish *et al*., 1995). There was a linear correlation ($r = 0.99$) for plasmid fluorescence intensity and $(TTAGGG)_n$ length with a slope of 47.7. The calibration-corrected telomere fluorescence intensity (ccTFI) of each telomere was calculated according to the formula ccTFI = (Bea1/Bea2)×(TFI/44.88); Bea1 = fluorescence intensity of beads when plasmids were analyzed; Bea2 = fluorescence intensity of beads when sample x was analyzed; TFI = unmodified fluorescence intensity of a telomere in sample x. Following this calibration, the fluorescence intensity of individual telomeres is expressed in TFU, in which one unit corresponds to 1 kb of TTAGGG repeats.

A restriction of this calibration method is that the actual telomeres are outside the range of $(TTAGGG)_n$ length of the plasmids. The assumption is made that the linear correlation obtained between fluorescence intensity and telomere insert size in the plasmids is maintained in the higher range in chromosomal DNA.

Histochemistry

Tissues were fixed in 4% paraformaldehyde and embedded in paraffin. Sections (5 μm) were stained with Harris hematoxylin and eosin.

[^{3}H]thymidine incorporation

A total of 2.5×10^5 splenocytes were resuspended in RPMI 1640 containing 10% FBS and 0.55 μM β-mercaptoethanol, and plated in round-bottomed 96-well plates. The mitogens utilized were anti-CD3 (1.5 μg/ml; PharMingen, San Diego, CA), concanavalin A (1.5 μg/ml; Sigma, St Louis, MO), LPS (10 μg/ml; Sigma), CD45R ligand (Pharmingen), ionomycin (1 μM; Sigma) and PMA (20 nM; Sigma). Following a 24 h pulse of ^{3}H-labeled thymidine, cells were harvested 48 h after mitogen addition onto glass fiber filter strips (Wallac, Turku, Finland) using an LKB Wallac 1295-001 Cell Harvester. The c.p.m. incorporated by each cell lysate were determined using an LKB 1205 Rackbeta Liquid Scintillation Counter (ICN, Costa Mesa, CA). Each sample was processed in triplicate and the standard deviations were calculated using Microsoft Excel.

FACS analyses

For the analysis of spleen cell subpopulations, we used FACS; 10^6 splenocytes were used for each analysis. Cells were washed in PBS with 1% FBS and incubated with chromogen-conjugated antibodies, including CD45–phycoreythrin (PE), IgM–PE, CD4–fluorescein isothiocyanate (FITC), CD3–FITC, B220–FITC, CD8-–FITC and CD62–PE. After incubation, cells were washed and analyzed by FACS. Flow cytometry was performed on a FACScan (Coulter, Miami, FL).

Hematology

Blood (100 μl) was obtained from the retro-orbital plexus of six different wild-type B6 mice and 12 G3 mTR$^{-/-}$ B6 mice at different ages, and placed in tubes containing 10% 0.5 M EDTA; hematological analysis was performed on a Technicon H.1E (Bayer Corporation).

Acknowledgements

Dedicated to the memory of Adela Gomis. We are indebted to Peter Lansdorp for providing the FISH analysis program and to Jessica Freire for her assistance in establishing the mouse generations. We thank Manuel Serrano, Carol Greider and Cathy Mark for critical reading of the manuscript. E.H. is supported by a predoctoral fellowship from the Department of Immunology and Oncology, Centro Nacional de Biotecnología-CSIC, Madrid. E.S. is supported by a predoctoral fellowship from the regional government of Madrid (CAM). Research at the laboratory of M.A.B. is funded by grants PM95-0014 and PM97-0133 from the Ministry of Education and Culture, Spain, by grant 08.1/0030/98 from the CAM, and by the Department of Immunology and Oncology. The Department of Immunology and Oncology was founded and is supported by the Spanish Research Council (CSIC) and Pharmacia & Upjohn.

References

Autexier,C. and Greider,C.W. (1996) Telomerase and cancer: revisiting the telomere hypothesis. *Trends Biochem.*, **21**, 387–391.

Blackburn,E.H. (1991) Structure and function of telomeres. *Nature*, **350**, 569–573.

Blasco,M.A., Funk,W.D., Villeponteau,B. and Greider,C.W. (1995) Functional characterization and developmental regulation of mouse telomerase RNA. *Science*, **269**, 1267–1270.

Blasco,M.A., Lee,H.-W., Hande,P., Samper,E., Lansdorp,P., DePinho,R. and Greider,C.W. (1997) Telomere shortening and tumor formation by mouse cells lacking telomerase RNA. *Cell*, **91**, 25–34.

Bodnar,A.G. *et al*. (1998) Extension of life-span by introduction of telomerase into normal human cells. *Science*, **279**, 349–352.

Chiu,C.P., Dragowska,W., Kim,N.W., Vaziri,H., Yui,J., Thomas,T.E., Harley,C.B. and Lansdorp,P.M. (1996) Differential expression of telomerase activity in hematopoietic progenitors from adult human bone marrow. *Stem Cells*, **14**, 239–48.

Collins,K., Kobayashi,R. and Greider,C.W. (1995) Purification of *Tetrahymena* telomerase and cloning of the genes for the two protein components of the enzyme. *Cell*, **81**, 677–686.

Counter,C.M., Avilion,A.A., LeFeuvre,C.E., Stewart,N.G., Greider,C.W., Harley,C.B. and Bacchetti,S. (1992) Telomere shortening associated with chromosome instability is arrested in immortal cells which express telomerase activity. *EMBO J.*, **11**, 1921–1929.

Feng,J. *et al*. (1995) The RNA component of human telomerase. *Science*, **269**, 1236–1241.

Gandhi,L. and Collins,K. (1998) Interaction of recombinant *Tetrahymena* telomerase proteins p80 and p95 with telomerase RNA and telomeric DNA substrates. *Genes Dev.*, **12**, 721–733.

Greenberg,R.A., Allsopp,R.C., Chin,L., Morin,G. and DePinho,R. (1998) Expression of mouse telomerase reverse transcriptase during development, differentiation and proliferation. *Oncogene*, **16**, 1723–1730.

Greider,C.W. (1996) Telomere length regulation. *Annu. Rev. Biochem.*, **65**, 337–365.

Greider,C.W. and Blackburn,E.H. (1989) A telomeric sequence in the RNA of *Tetrahymena* telomerase required for telomere repeat synthesis. *Nature*, **337**, 331–337.

Hande,P., Samper,E., Lansdorp,P. and Blasco,M.A. (1999) Telomere length dynamics and chromosomal instability in cells derived from telomerase null mice. *J. Cell Biol.*, **144**, 589–601.

Hanish,J.P., Yanowitz,J.L. and de Lange,T. (1995) Stringent sequence requirements for the formation of human telomeres. *Proc. Natl Acad. Sci. USA*, **91**, 8861–8865.

Harley,C.B., Futcher,A.B. and Greider,C.W. (1990) Telomeres shorten during aging of human fibroblasts. *Nature*, **345**, 458–460.

Harrington,L., Zhou,W., McPhail, T, Oulton,R., Yeung,D., Mar,V., Bass,M.B. and Robinson,W. (1997a) Human telomerase contains evolutionarily conserved catalytic and structural subunits. *Genes Dev.*, **11**, 3109–3115.

Harrington,L., McPhail,T., Mar,V., Zhou,W., Oulton,R., Bass,M.B., Arruda,I. and Robinson,M.O. (1997b) A mammalian telomerase-associated protein. *Science*, **275**, 973–977.

Herrera,E., Samper,E. and Blasco,M.A (1999) Telomere shortening in mTR$^{-/-}$ embryos is associated with failure to close the neural tube. *EMBO J.*, **18**, 1172–1181.

Hiyama,K., Hirai,Y., Kyoizumi,S., Akiyama,M., Hiyama,E., Piatyszek, M.A., Shay,J.W., Ishioka,S. and Yamakido,M. (1995) Activation of telomerase in human lymphocytes and hematopoietic progenitor cells. *J. Immunol.*, **155**, 3711–3715.

Jiang,X.-R. *et al*. (1999) Telomerase expression in human somatic cells does not induce changes associated with a transformed phenotype. *Nature Genet.*, **21**, 111–114.

Kilian,A., Bowtell,D.D.L., Abud,H.E., Hime,G.R., Venter,D.J., Keese,P.K., Duncan,E.L., Reddel,R.R. and Jefferson,R.A. (1997) Isolation of a candidate human telomerase catalytic subunit gene, which reveals complex splicing patterns in different cell types. *Hum. Mol. Genet.*, **6**, 2011–2019.

Kiyono,T., Foster,S.A., Koop,J.I., McDougall,J.K., Galloway,D.A. and Klingelhutz,A.J. (1998) Both Rb/p16^{INK4a} inactivation and telomerase activity are required to immortalize human epithelial cells. *Nature*, **396**, 84–88.

Lee,H.-W., Blasco,M.A., Gottlieb,G.J., Horner.,J.W., Greider,C.W. and DePinho,R.A. (1998) Essential role of mouse telomerase in highly proliferative organs. *Nature*, **392**, 569–574.

Lingner,J., Hughes,T.R., Schevchenko,A., Mann,M., Lundblad,V. and Cech,T. (1997) Reverse transcriptase motifs in the catalytic subunit of telomerase. *Science*, **276**, 561–567.

Martens,U.M., Zijlmans,J.M., Poon,S., Dragowska,W., Yui,J., Chavez,E., Ward,R. and Lansdorp,P.M. (1998) Short telomeres on human chromosome 17p. *Nature Genet.*, **18**, 76–80.

Martín-Rivera,L., Herrera,E., Albar,J.P. and Blasco,M.A. (1998) Expression of mouse telomerase catalytic subunit in embryos and adult tissues. *Proc. Natl Acad. Sci. USA*, **95**, 10471–10476.

McEachern,M.J. and Blackburn,E.H. (1995) Runaway telomere elongation caused by telomerase RNA gene mutations. *Nature*, **376**, 403–409.

Meyerson,M. *et al*. (1997) hEST2, the putative human telomerase catalytic subunit gene, is upregulated in tumor cells and during immortalization. *Cell*, **90**, 785–795.

Mohr *et al*. (1996) *Pathobiology of the Aging Mouse*. Vol. 2. ILSI Press.

Morales,C.P., Holt,S.E., Ouellette,M., Kaur,K.J., Yan,Y., Wilson,K.S., White,M.A., Wright,W.E. and Shay,J.W. (1999) Absence of cancer-associated changes in human fibroblasts immortalized with telomerase. *Nature Genet.*, **21**, 115–118.

Nakamura,T.M., Morin,G.B., Chapman,K.B., Weinrich,S.L., Andrews, W.H., Lingner,J., Harley,C.B. and Cech,T. (1997) Telomerase catalytic subunit homologs from fission yeast and human. *Science*, **277**, 955–959.

Nakamura,T.M., Cooper,J.P. and Cech,T. (1998) Two modes of survival of fission yeast without telomerase. *Science*, **282**, 493–496.

Nakayama,J., Saito,M., Nakamura,H., Matsuura,A. and Ishikawa,F. (1997) *TLP1*: a gene encoding a protein component of mammalian telomerase is a novel member of WD repeat family. *Cell*, **88**, 875–884.

Niida,H., Matsumoto,T., Satoh,H., Shiwa,M., Tokutake,Y., Furuici,Y. and Shinkai,Y. (1998) Severe growth defect in mouse cells lacking the telomerase RNA component. *Nature Genet.*, **19**, 203–206.

Nistal,M., Paniagua,R., Abaurrea,M.A. and Santamaría,L. (1982) Hyperplasia and immature appearance of Sertoli-cells in primary testicular disorders. *Hum. Pathol.*, **13**, 3–12.

Nugent,C.I. and Lundblad,V. (1998) The telomerase reverse transcriptase: components and regulation, *Genes Dev.*, **12**, 1073–1085.

Rudolph,K.L., Chang,S., Lee,H.-W., Blasco,M.A., Gottlieb,G., Greider, W.C. and DePinho,R.A. (1999) Longevity, stress response and cancer in aging telomerase deficient mice. *Cell*, **96**, 701–712.

Singer,M.S. and Gottschling,D.E. (1994) TLC1: template RNA component of the *Saccharomyces cerevisiae* telomerase. *Science*, **266**, 387–388.

Smith,C.A., Andrews,C.M., Collard,J.K., Hall,D.E., Walker,A.K. and Wolfe,M. (1994) Color Atlas of Comparative Diagnostic and Experimental Hematology. Wolfe Publishing, London, UK.

Stevens,A. and Lowe,J. (1997) *Human Histology*, 2nd Edn. Times Mirror International Publishers Ltd, UK.

Takano,H. and Abe,K. (1987) Age-related histologic changes in the adult mouse testis. *Arch. Histol. Japan*, **50**, 533–544.

Vaziri,H., Schachter,F. and Uchida,I. (1993) Loss of telomeric DNA during aging of normal and trisomy 21 human lymphocytes. *Am. J. Hum. Genet.*, **52**, 661–667.

Wang,J., Xie,L.Y., Allan,S., Beach,D. and Hannon,G.J. (1998) Myc activates telomerase. *Genes Dev.*, **12**,1769–1774.

Wick,G. and Grubeck-Loebenstein,B. (1997) Primary and secondary alterations of immune reactivity in the elderly: impact of dietary factors and disease. *Immunol. Rev.*, **160**, 171–184.

Zijlmans,J.M., Martens,U.M., Poon,S., Raap,A.K., Tanke,H.J., Ward, R.K. and Lansdorp,P.M. (1997) Telomeres in the mouse have large inter-chromosomal variations in the number of T2AG3 repeats. *Proc. Natl Acad. Sci. USA*, **94**, 7423–7428.

Received February 24, 1999; revised and accepted April 8, 1999